Journal of Materials Chemistry A

PAPER

View Article Online
View Journal | View Issue

Cite this: J. Mater. Chem. A, 2019, 7, 10723

Realizing facile regeneration of spent $NaBH_4$ with Mg–Al alloy†

Hao Zhong,[a] Liuzhang Ouyang, *[ab] Meiqin Zeng,[a] Jiangwen Liu,[a] Hui Wang,[a] Huaiyu Shao, *[c] Michael Felderhoff *[d] and Min Zhu [a]

Received 21st January 2019
Accepted 28th March 2019

DOI: 10.1039/c9ta00769e

rsc.li/materials-a

The regeneration of sodium borohydride ($NaBH_4$) is crucial to form a closed cycle after it either supplies hydrogen energy *via* a hydrolysis process or provides energy through electron transfer at the anode of direct borohydride fuel cells (DBFCs). In both of these cases, the spent fuels are $NaB(OH)_4$ from $NaBO_2$ aqueous solution. However, the current regeneration process from $(NaB(OH)_4)\cdot xH_2O$ to form $NaBH_4$ by reduction reaction and calcination at high temperature with metal hydrides as reducing agents is very expensive. In this work, we developed a simple regeneration process *via* ball milling with Mg–Al alloys as the reducing agent for $NaB(OH)_4$ under an argon atmosphere. Under optimized conditions, a high yield of about 72% of $NaBH_4$ could be obtained. Mechanistic study showed that all the hydrogen atoms from $NaB(OH)_4$ remain in $NaBH_4$ and no additional hydrogen sources are needed for the reduction process. The inexpensive Mg–Al alloy works as a reducing agent transforming the H^+ to H^- in $NaBH_4$. This approach demonstrates a ~20-fold cost reduction compared with the method using metal hydrides. This opens the door to the commercial implementation of simple ball milling processes for the regeneration of spent $NaBH_4$ from $NaB(OH)_4$ with cheap reducing agents.

1. Introduction

Fuel cells provide a promising alternative technology for electrical power generation from renewable energy carriers, for instance, hydrogen energy.[1] However, currently the fuel supply is still one of the biggest hindrances for worldwide application of mobile fuel cell technologies.[2,3] Hydrogen supply *via* hydrolysis of sodium borohydride ($NaBH_4$)[4] or direct borohydride fuel cells (DBFCs) both have great potential as possible solutions.[5] However, both of these technologies suffer from the high cost of $NaBH_4$ as well as difficulties in the regeneration of the spent fuel.[6,7] Therefore, a high-efficiency and low-cost approach for a simple regeneration process for spent $NaBH_4$ is highly desirable. This could be the key step and enabling technology for further distribution of $NaBH_4$-powered fuel cell applications.

The spent fuel from $NaBH_4$ hydrolysis is confirmed by the following hydrolysis reaction:

$$NaBH_4 + (2 + x)H_2O \rightarrow NaBO_2\cdot xH_2O + 4H_2 + \text{heat} \quad (1)$$

where x is the hydration factor.[8] However, it should be noted that the spent fuel is normally hydrated sodium metaborate ($NaBO_2$) or its aqueous solution after the hydrolysis.[9] The actual formulae of $NaBO_2\cdot 2H_2O$ and $NaBO_2\cdot 4H_2O$ are $NaB(OH)_4$ and $NaB(OH)_4\cdot 2H_2O$, respectively, according to the chemical structures.[10] In DBFCs, $NaBH_4$ is oxidized at the anode according to the following reaction:

$$BH_4^- + 8OH^- \rightarrow BO_2^- + 6H_2O + 8e^-, \quad E^0 = -1.24\ \text{V}\ \textit{vs.}\ \text{SHE} \quad (2)$$

The spent fuel from the anode reaction is $B(OH)_4^-$ and H_2O, which are also generated as an aqueous solution of $NaBO_2$.[7,11] From the $NaBO_2$ aqueous solution, $NaB(OH)_4\cdot 2H_2O$ or $NaB(OH)_4$ can be obtained *via* drying at temperatures of <54 °C or 54–110 °C, respectively, while dehydrated $NaBO_2$ can be formed after treatment at temperatures >350 °C.[12] Over the past few decades, a great deal of effort has been made toward dehydrated $NaBO_2$ reduction. With a calcination treatment at 550 °C, MgH_2 reduced the dehydrated $NaBO_2$ to $NaBH_4$ under hydrogen pressure.[13] Ball milling with metal hydrides at near

[a]School of Materials Science and Engineering, Guangdong Provincial Key Laboratory of Advanced Energy Storage Materials, South China University of Technology, Guangzhou, 510641, People's Republic of China. E-mail: meouyang@scut.edu.cn

[b]China-Australia Joint Laboratory for Energy & Environmental Materials, Key Laboratory of Fuel Cell Technology of Guangdong Province, Guangzhou, 510641, People's Republic of China

[c]Joint Key Laboratory of the Ministry of Education, Institute of Applied Physics and Materials Engineering (IAPME), University of Macau, Macau SAR, China. E-mail: hshao@um.edu.mo

[d]Max-Planck-Institut für Kohlenforschung, 45470 Mülheim an der Ruhr, Germany. E-mail: felderhoff@mpi-muelheim.mpg.de

† Electronic supplementary information (ESI) available: XRD analysis of the raw materials; XRD analysis of the ball milled products; XPS analysis of the ball milled raw material; cost calculation of raw materials for $NaBH_4$ produced by different approaches. See DOI: 10.1039/c9ta00769e

room temperature can also achieve the reduction under an argon atmosphere with a $NaBH_4$ yield of over 70%.[14–16] However, the synthesis of metal hydrides at high temperature could be one important factor in the energy consumption and cost. Without the use of metal hydrides, high-temperature annealing treatment under hydrogen pressure for Mg,[13,17] Mg and Si[13] or transition metals (Fe, Co or Ni)[18,19] mixed with dehydrated $NaBO_2$ is another reduction technique. However, this high-temperature dehydration of $NaBO_2$ is also energy consuming and additional hydrogen supply is needed, which increases the costs of the regeneration process (hydrogen from renewable sources, like water splitting, or unsustainably from fossil fuels). Direct reduction of hydrated $NaBO_2$ with Mg by annealing at 3 MPa hydrogen pressure may be an option, but the yield is only 12.3% of $NaBH_4$.[20] Therefore, an innovative low-cost and high-efficiency approach for $NaBH_4$ regeneration is of great importance and is urgently required.

Herein, instead of only Mg, we introduce aluminum (Al) to the reduction process of hydrated $NaBO_2$ because it can offer more electrons than Mg but with similar reducibility, which may further decrease the cost and increase the yield of the process. In addition, Mg and Al are relatively soft metals, making the ball milling process less efficient. Thus, magnesium aluminum alloy ($Mg_{17}Al_{12}$) was chosen as a reducing agent in this work. The alloy was used to react with hydrated $NaBO_2$ *via* ball milling under an argon atmosphere in order to regenerate $NaBH_4$. During the ball milling process, oxide layers on the alloy will be destroyed and fresh surfaces will be produced continuously. This will increase the overall kinetics of the regeneration process.

In this process, the $Mg_{17}Al_{12}$ alloy offers a high $NaBH_4$ yield and a low cost, while the hydrated $NaBO_2$ provides a self-sufficient hydrogen source with no need for any additional hydrogen input. Furthermore, the unnecessity of drying at high temperature (>350 °C) may greatly reduce energy consumption during the regeneration process. Therefore, this approach for regeneration of $NaBH_4$ may be a very promising solution for future energy supply technologies.

2. Experimental

2.1 Chemicals

$Mg_{17}Al_{12}$ was purchased from Aike Reagent (China), while $NaB(OH)_4$ was obtained by drying $(NaB(OH)_4)\cdot 2H_2O$ (>99%, Sigma-Aldrich) for 12 h. Ethylenediamine (≥99%) was purchased from Sigma-Aldrich. The chemicals for quantification, potassium iodate (KIO_3, AR grade), H_2SO_4 (98%), NaOH (≥99%), starch indicator (≥99%), and sodium thiosulfate solution ($Na_2S_2O_3$, 1 M, AR grade) were purchased from Aladdin, and potassium iodide (KI, ≥99%) was purchased from TCI. The $Mg_{17}Al_{12}$ and the generated $NaB(OH)_4$ were stored and handled in an argon-filled glove box (Mikrouna, China). The oxygen and water concentrations in the glove box were always below 1 ppm.

2.2 $NaBH_4$ regeneration

For a typical experiment, a total 1 g of $Mg_{17}Al_{12}$ and $NaB(OH)_4$ with different mole ratios and 50 g of steel balls (ball to powder ratio of 50 : 1, 4 steel balls of 10 mm and 68 steel balls of 6 mm) were mixed and loaded in the milling vial in the glove box. Then, the ball milling reactions were carried out in a shaker mill (QM-3C, Nanjing, China) at 1200 cycles per min (cpm).

2.3 Purification and quantification

20 mL of ethylenediamine was used to extract $NaBH_4$ from the ball milled products. The turbid solution was then filtered *via* a polytetrafluoroethylene filter. The clear $NaBH_4$ solution was dried using a freeze dryer (Martin Christ, Alpha 1-2LD Plus, Germany) to obtain $NaBH_4$ as a white powder and the waste solvent (ethylenediamine) was collected in the cold trap. The purified $NaBH_4$ was quantified by the iodate method.[21] The yield of NaBH4 was calculated according to the following equation:

$$\text{Yield} = \frac{\text{obtained NaBH}_4\text{ mass}}{\text{theoretical NaBH}_4\text{ mass}} \times 100\% \quad (3)$$

2.4 Hydrolysis process

The hydrolysis test was conducted using the hydrolysis apparatus introduced here.[22] In each hydrolysis experiment, 0.1 g of $NaBH_4$ was used to react with 0.225 mL of a 5 wt% aqueous solution of $CoCl_2$ at room temperature and the hydrogen generation curves were automatically collected.

2.5 Characterization

The phase composition was measured by X-ray diffractometer (XRD, Rigaku MiniFlex 600) with Cu Kα radiation ($\lambda = 1.5406$ Å) at 45 kV and 40 mA. Because both the raw materials and milling products are air sensitive, liquid paraffin was used to protect the XRD samples from the air. The chemical bonds of the products were measured by Fourier-transform infrared spectroscopy (FTIR, IS50, Nicolet) in transmission mode. Potassium bromide (KBr) pellets for FTIR measurements were prepared in the glove box with a sample to KBr ratio of 1 : 99. The ball milling products were also characterized by solid-state ^{11}B magic-angle spinning nuclear magnetic resonance (MAS NMR) spectroscopy (AVANCE III HD 400, Bruker). Scanning electron microscopy (SEM; Supra-40, Zeiss) was used to characterize the morphology of the $NaBH_4$.

3. Results and discussion

3.1 $NaBH_4$ synthesis

For the $NaBH_4$ regeneration, a mixture of $Mg_{17}Al_{12}$ alloy and $NaB(OH)_4$ in a molar ratio of 4 : 35 was mechanochemically treated with a ball to powder ratio of 50 : 1 at 1200 cpm under an argon atmosphere. The XRD curves of the raw materials are shown in Fig. S1.† Fig. 1a shows the XRD curves of the generated $NaBH_4$ after milling depending on the milling time. It can be seen that the raw materials ($Mg_{17}Al_{12}$ and $(NaB(OH)_4)$) lose their intensity gradually with increasing milling time. The (200) diffraction peak of $NaBH_4$ at around 28.9° in the XRD pattern confirms the generation of $NaBH_4$ after 2 hours of milling. With the further increase of the milling time, the diffraction peak of

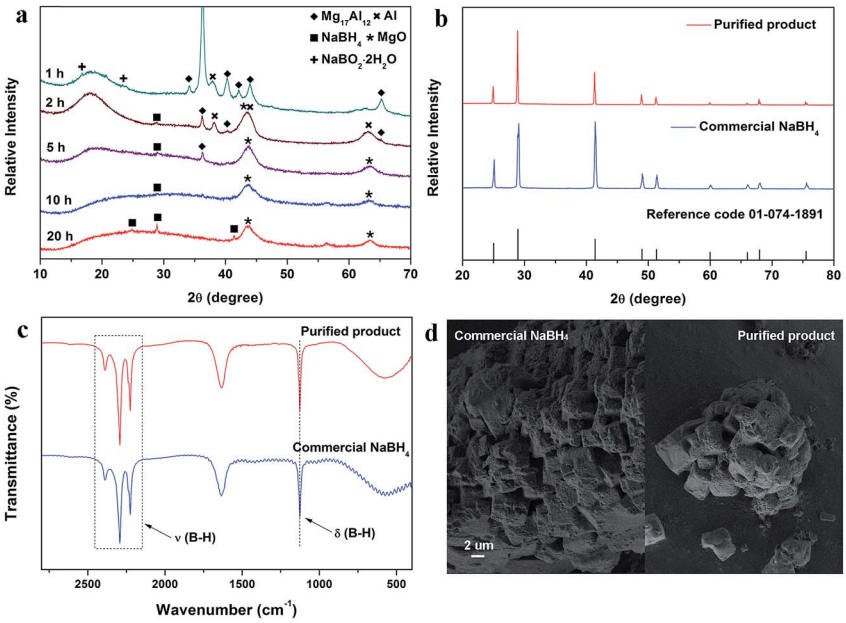

Fig. 1 (a) XRD patterns of the 5, 7.5, 10 and 20 h ball milled products of $Mg_{17}Al_{12}$ and $NaB(OH)_4$ mixtures (in a 4 : 35 molar ratio). (b) XRD patterns of the purified product (red line) and commercial $NaBH_4$ (blue line). (c) FTIR spectra of the purified product (red line) and the commercial $NaBH_4$ (blue line). (d) SEM images of the commercial $NaBH_4$ (left) and the purified product (right).

$NaBH_4$ becomes stronger after 5 h of milling but the intensity decrease after 10 h of milling, which may result from the combination effect of amorphization and $NaBH_4$ generation during ball milling. After 20 h of milling, the (111) and (220) diffraction peaks of $NaBH_4$ appear at around 25.1° and 41.4° with the sharper (200) diffraction peak at 28.9° because of the crystallization.[23]

To remove the byproducts from the powder after 5 h of milling and obtain high-purity $NaBH_4$, the ball milling products were further purified. Fig. 1b presents the XRD curved for the purified $NaBH_4$ product and the commercial material. As compared to the curve from commercial $NaBH_4$, the similar diffraction pattern of the purified $NaBH_4$ and the sharp (111), (200), (220), (311), (222), (400), (331) and (420) diffraction peaks[14,15] indicate the successful generation of high-purity $NaBH_4$ phase. No other reflections can be detected from the XRD pattern. From the FTIR spectra of these two samples shown in Fig. 1c, the bonds of the purified $NaBH_4$ were further analyzed. The stretching (2200–2400 cm^{-1}) and bending (1125 cm^{-1}) vibrations of B–H appear in the spectrum of the purified $NaBH_4$,[14,16] which are similar to the vibrations of commercial $NaBH_4$. Therefore, we may conclude that the regenerated $NaBH_4$ with a similar crystal structure and bonding features to the commercial $NaBH_4$ was regenerated by the reaction between $Mg_{17}Al_{12}$ and $NaB(OH)_4$ *via* ball milling. This method not only avoids the high-temperature process at 350 °C for $NaB(OH)_4$ reduction, but also realizes the complete H supply for the regenerated $NaBH_4$ from the $[OH]^-$ group of $NaB(OH)_4$. Fig. 1d shows the SEM images of the purified and the commercial $NaBH_4$. The grain-like surface structure of the purified $NaBH_4$ is quite similar to that of the commercial $NaBH_4$, which indicates that the regenerated $NaBH_4$ has a similar surface morphology to that of the commercial $NaBH_4$.

3.2 Yield

Fig. 2a presents the yields of high-purity $NaBH_4$ prepared from the raw materials $Mg_{17}Al_{12}$ and $NaB(OH)_4$ in molar ratios of 4 : 35 and 4 : 17 depending on the milling time. Quantification of the pure $NaBH_4$ was done with the iodate method. For the 4 : 35 ratio, the $NaBH_4$ yield after 5 h of milling was 20% and the yields increased with the milling time. After 20 h of milling, the yield reached 37%. As known from previous studies, the relation of $NaB(OH)_4$ to the reduction compound has an important influence on the $NaBH_4$ yield.[24–26] It was further optimized by varying the molar ratio of $Mg_{17}Al_{12}$ and $NaB(OH)_4$ (raw materials ratio). Fig. 2b shows the $NaBH_4$ yields depending for the raw materials ratio range from 4 : 35 to 4.5 : 17 after 10 and 20 h of ball milling. For both of the milling durations, the $NaBH_4$ yield first increases then decreases with increasing raw materials ratio. However, the highest yield after 10 h of ball milling was 54% with the raw materials ratio of 3.5 : 17, while for 20 h of milling the yield was 72% when the raw materials ratio was 4 : 17. It should be noted that the highest $NaBH_4$ yield in this work of 72% is higher than the yield of the Mg and $NaB(OH)_4$ system in our previous study[27] and also approaches the yields from other reports of $NaBH_4$ regeneration *via* MgH_2 and $NaBO_2$.[14–16] The yields for the shorter milling times of the products with a raw materials ratio of 4 : 17 are presented in Fig. 2a. The yields for 5 h (5%) and 7.5 h (9%) milling times are lower than that with the 4 : 35 raw materials molar ratio, and the diffraction peaks of $NaBH_4$ cannot be found in the XRD results (Fig. S2†). Diffraction peaks for $NaBH_4$ appear in the pattern of the product after 5 h of ball milling, while the peak

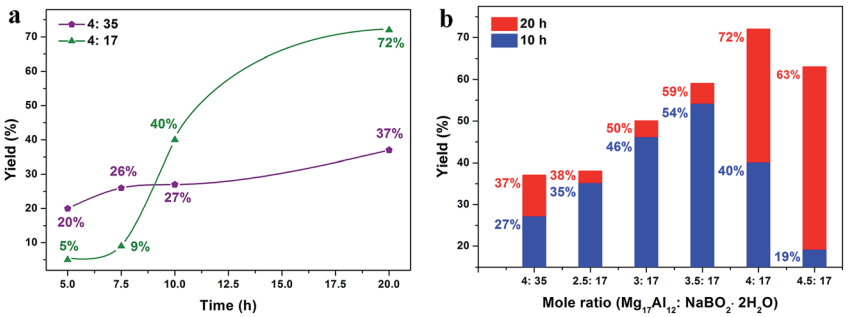

Fig. 2 (a) Yields of the ball milled products of $Mg_{17}Al_{12}$ and $NaB(OH)_4$ mixtures (in 4 : 35 and 4 : 17 molar ratios) for different milling times. (b) Yields of the 10 and 20 h ball milled products of $Mg_{17}Al_{12}$ and $NaB(OH)_4$ mixtures with different mole ratios.

for $NaBH_4$ appears in the pattern of the product with the 4 : 35 raw materials ratio only after 2 h of ball milling (Fig. 1a). Strong crystallization of $NaBH_4$ happens when the ball milling time is increased to 20 h. The diffraction peaks for $NaBH_4$ in the product with the raw materials ratio of 4 : 17 are much sharper (Fig. S2†).

3.3 Reaction mechanism

To clarify the reaction mechanism between $Mg_{17}Al_{12}$ alloy and $NaB(OH)_4$, the products obtained with different milling times were also investigated and characterized by FTIR, as shown in Fig. 3a. According to the XRD patterns in Fig. 1a, the (111) diffraction peak of Al at 38.4° and the (200) diffraction peak of MgO at 42.9° imply the generation of Al and MgO after 1 and 2 h of milling. After 1 h of milling, the formation of $NaBH_4$ could be verified by the appearance of B–H vibrations in the FTIR spectrum in Fig. 3a and the $[BH_4]^-$ resonance from Fig. 3b. According to the NMR spectra (Fig. 3b), $[B(OH)_4]^-$ is gradually reduced to $[BH_4]^-$ in this process. Therefore, the first step of the regeneration process can be described by the following reaction:

$$Mg_{17}Al_{12} + NaB(OH)_4 \rightarrow MgO + Al + NaBH_4 \quad (4)$$

The diffraction peaks of Al then disappear after 5 h of milling, which indicates that Al may become amorphous or work as a reducing agent and react with $NaB(OH)_4$ during the ball milling. Because Al was generated after 1 h of milling and could react with $NaB(OH)_4$, to further confirm the reaction, the product was characterized by XPS and the results are shown in Fig. 3c, which may provide more evidence. The only peak that appears at 74.30 eV in the spectrum is indexed to Al^{3+}, while the

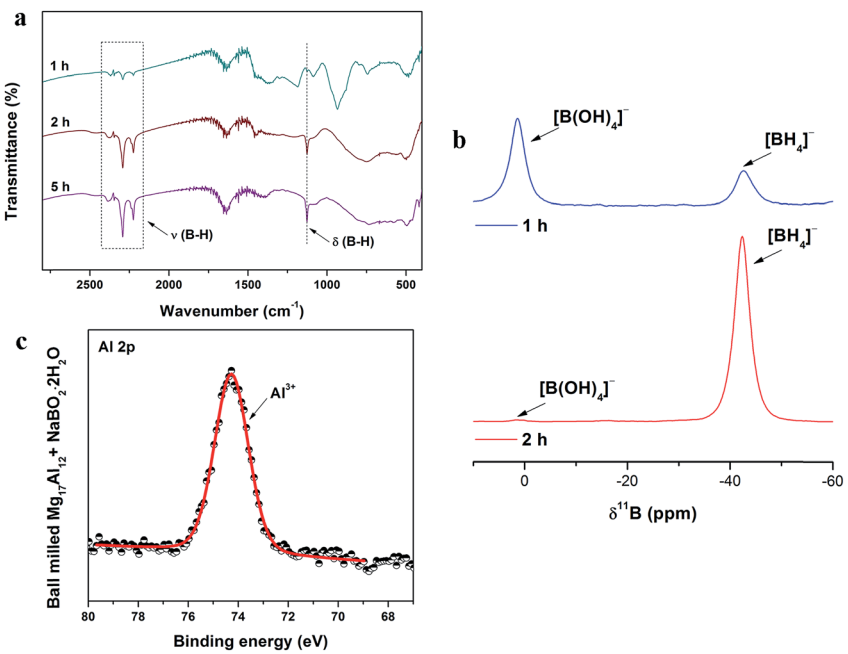

Fig. 3 (a) FTIR spectra of the 1, 2 and 5 h ball milled products of $Mg_{17}Al_{12}$ and $NaB(OH)_4$ mixtures (in a molar ratio of 4 : 35). (b) ^{11}B NMR spectra of the 1 and 2 h ball milled products of $Mg_{17}Al_{12}$ and $NaB(OH)_4$ mixtures (in a 4 : 35 molar ratio). (c) XPS spectra of Al 2p of the 1 h ball milled products of $Mg_{17}Al_{12}$ and $NaB(OH)_4$ mixtures (in a 4 : 35 molar ratio).

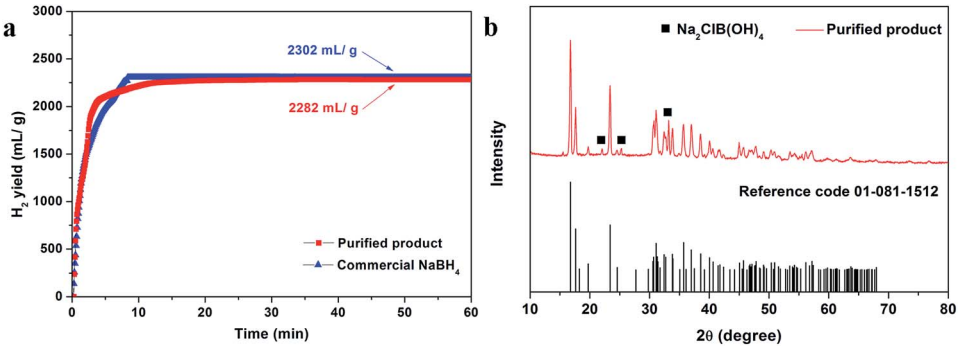

Fig. 4 (a) Hydrolysis curves of the purified product (red line) and commercial $NaBH_4$ (blue line). (b) XRD pattern of the hydrolysis byproduct of the purified product.

peak belonging to Al^0 in $Mg_{17}Al_{12}$ can be found in the spectrum for $Mg_{17}Al_{12}$ (Fig. S3†) milled with the same parameters. This evidence indicates that Al reacts with $NaB(OH)_4$ in this reaction. To further unveil the reaction mechanism, pure Al-metal and $NaB(OH)_4$ in a molar ratio of 24 : 9 were ball milled for 5 h with the same other milling parameters. Only diffraction peaks from Al-metal were found in the XRD pattern (Fig. S4a†) while on the other hand B–H vibrations appeared in the FTIR spectrum (Fig. S4b†). This demonstrates that even Al-metal can react with $NaB(OH)_4$ producing $NaBH_4$. Considering that Mg transfers to MgO in this system, it can be assumed that the byproduct is Al_2O_3 but not $Al(OH)_3$, which may be amorphous so that its diffraction peaks cannot be observed in the XRD patterns. Therefore, the reaction of the second step is described as:

$$Al + NaB(OH)_4 \rightarrow Al_2O_3 + NaBH_4 \quad (5)$$

Fig. 3b shows the solid-state ^{11}B MAS NMR spectra of boron compounds produced during ball milling with different milling times. When the milling time changes from 1 to 2 h, the intensity of the $[B(OH)_4]^-$ resonance decreases sharply, while the intensity of the $[BH_4]^-$ resonance increases, indicating the conversion from $[B(OH)_4]^-$ to $[BH_4]^-$. Owing to the self-supplied H from the $[OH]^-$ group in the raw material of $NaB(OH)_4$, and the avoidance of high-temperature dehydration in this system, the cost of the regenerated $NaBH_4$ is significantly reduced, benefitting from the use of the $Mg_{17}Al_{12}$ alloy. From calculations for the price of the raw materials, the expected cost of this process is ~20 fold lower than the method using MgH_2 and dehydrated $NaBO_2$ as raw materials (Table S1†). An approximately 25% reduction in the cost of the raw materials is also achieved compared with the commercial method.

3.4 Hydrolysis

The generation of hydrogen from $NaBH_4$ *via* hydrolysis was also examined to confirm its properties. Here, a low-cost and effective non-noble metal catalyst, cobalt chloride ($CoCl_2$),[28] was used in the hydrolysis process. According to the hydrogen generation curves in Fig. 4a, the regenerated $NaBH_4$ shows fast hydrogen generation kinetics, although with a little lower final hydrogen generation content than that of the commercial $NaBH_4$. Nevertheless, around 2215 mL g^{-1} hydrogen can be generated within 10 min, with a conversion rate of about 86%. After the hydrolysis, the byproduct was collected and placed in ambient condition for 48 h before XRD measurement. In the XRD pattern (Fig. 4b), the low intensity diffraction peaks located at 22.0°, 25.2° and 33.2° are indexed to the (101), (111) and (211) of $Na_2ClB(OH)_4$, while other peaks are similar to those of $NaB(OH)_4$. We can conclude here that the $NaB(OH)_4$ is the main phase of the byproduct, which can be regenerated by the above method.

4. Conclusion

In summary, $NaB(OH)_4$ can be successfully reduced with $Mg_{17}Al_{12}$ alloy *via* ball milling to realize a very easy regeneration process for spent $NaBH_4$. Using the inexpensive $Mg_{17}Al_{12}$ alloy, a H^--anion in the regenerated $NaBH_4$ is directly transferred from the $[OH]^-$ group to H^-. The yield in $NaBH_4$ reaches 72%, which results from the reducibility of Mg and also Al-metal. During the reduction process, firstly the $Mg_{17}Al_{12}$ alloy reacts with $NaB(OH)_4$ and generates $NaBH_4$, MgO and Al-metal. Afterwards, the Al-metal reacts with residual $NaB(OH)_4$ and produces $NaBH_4$ and Al_2O_3. Since both metals of the cheap $Mg_{17}Al_{12}$ alloy can act as reducing agents, the commercial cost of this regeneration method is further reduced by a factor of ~20 compared to regeneration methods using metal hydrides as the reducing agent. This new method holds promise for use as a commercial regeneration process and could open the door for broad applications of energy supply from $NaBH_4$.

Conflicts of interest

There are no conflicts to declare.

Acknowledgements

This work was supported by the Foundation for Innovative Research Groups of the National Natural Science Foundation of China (No. NSFC51621001) and National Natural Science Foundation of China Projects (No. 51431001 and 51771075). Author Ouyang also thanks Guangdong Province Universities

and Colleges Pearl River Scholar Funded Scheme (2014). Shao acknowledges Macao Science and Technology Development Fund (FDCT) for project 118/2016/A3.

References

1 U. Eberle, B. Muller and R. von Helmolt, *Energy Environ. Sci.*, 2012, **5**, 8780–8798.
2 S. Guo, J. Sun, Z. Zhang, A. Sheng, M. Gao, Z. Wang, B. Zhao and W. Ding, *J. Mater. Chem. A*, 2017, **5**, 15879–15890.
3 S. Park, J. M. Vohs and R. J. Gorte, *Nature*, 2000, **404**, 265.
4 D. M. F. Santos and C. A. C. Sequeira, *Renewable Sustainable Energy Rev.*, 2011, **15**, 3980–4001.
5 G. Rostamikia and M. J. Janik, *Energy Environ. Sci.*, 2010, **3**, 1262–1274.
6 U. B. Demirci, O. Akdim and P. Miele, *Int. J. Hydrogen Energy*, 2009, **34**, 2638–2645.
7 I. Merino-Jiménez, C. Ponce de León, A. A. Shah and F. C. Walsh, *J. Power Sources*, 2012, **219**, 339–357.
8 A. Marchionni, M. Bevilacqua, J. Filippi, M. G. Folliero, M. Innocenti, A. Lavacchi, H. A. Miller, M. V. Pagliaro and F. Vizza, *J. Power Sources*, 2015, **299**, 391–397.
9 M. A. Budroni, S. Garroni, G. Mulas and M. Rustici, *J. Phys. Chem. C*, 2017, **121**, 4891–4898.
10 L. J. Csetenyi, F. P. Glasser and R. A. Howie, *Acta Crystallogr., Sect. C: Cryst. Struct. Commun.*, 1993, **49**, 1039–1041.
11 Z. P. Li, B. H. Liu, K. Arai and S. Suda, *J. Alloys Compd.*, 2005, **404–406**, 648–652.
12 A. M. Beaird, P. Li, H. S. Marsh, W. A. Al-Saidi, J. K. Johnson, M. A. Matthews and C. T. Williams, *Ind. Eng. Chem. Res.*, 2011, **50**, 7746–7752.
13 Y. Kojima and T. Haga, *Int. J. Hydrogen Energy*, 2003, **28**, 989–993.
14 C.-L. Hsueh, C.-H. Liu, B.-H. Chen, C.-Y. Chen, Y.-C. Kuo, K.-J. Hwang and J.-R. Ku, *Int. J. Hydrogen Energy*, 2009, **34**, 1717–1725.
15 L. Kong, X. Cui, H. Jin, J. Wu, H. Du and T. Xiong, *Energy Fuels*, 2009, **23**, 5049–5054.
16 Ç. Çakanyıldırım and M. Gürü, *Renewable Energy*, 2010, **35**, 1895–1899.
17 Z. P. Li, B. H. Liu, J. K. Zhu, N. Morigasaki and S. Suda, *J. Alloys Compd.*, 2007, **437**, 311–316.
18 B. Liu, *Int. J. Hydrogen Energy*, 2008, **33**, 1323–1328.
19 B. H. Liu, Z. P. Li and S. Suda, *J. Alloys Compd.*, 2009, **474**, 321–325.
20 B. H. Liu, Z. P. Li and J. K. Zhu, *J. Alloys Compd.*, 2009, **476**, L16–L20.
21 D. A. Lyttle, E. H. Jensen and W. A. Struck, *Anal. Chem.*, 1952, **24**, 1843–1844.
22 L. Ouyang, M. Ma, M. Huang, R. Duan, H. Wang, L. Sun and M. Zhu, *Energies*, 2015, **8**, 4237.
23 C. Suryanarayana, *Prog. Mater. Sci.*, 2001, **46**, 1–184.
24 H. Zhong, L. Z. Ouyang, J. S. Ye, J. W. Liu, H. Wang, X. D. Yao and M. Zhu, *Energy Storage Mater.*, 2017, **7**, 222–228.
25 W. Chen, L. Z. Ouyang, J. W. Liu, X. D. Yao, H. Wang, Z. W. Liu and M. Zhu, *J. Power Sources*, 2017, **359**, 400–407.
26 H. Zhong, L. Ouyang, J. Liu, C. Peng, X. Zhu, W. Zhu, F. Fang and M. Zhu, *J. Power Sources*, 2018, **390**, 71–77.
27 L. Ouyang, W. Chen, J. Liu, M. Felderhoff, H. Wang and M. Zhu, *Adv. Energy Mater.*, 2017, 1700299.
28 H.-B. Dai, G.-L. Ma, X.-D. Kang and P. Wang, *Catal. Today*, 2011, **170**, 50–55.